Check for updates

View Article Online
View Journal

Journal of Materials Chemistry C

Materials for optical, magnetic and electronic devices

Accepted Manuscript

This article can be cited before page numbers have been issued, to do this please use: S. Prasad, C. M. G. Araujo and E. Moons, *J. Mater. Chem. C*, 2026, DOI: 10.1039/D5TC03779D.

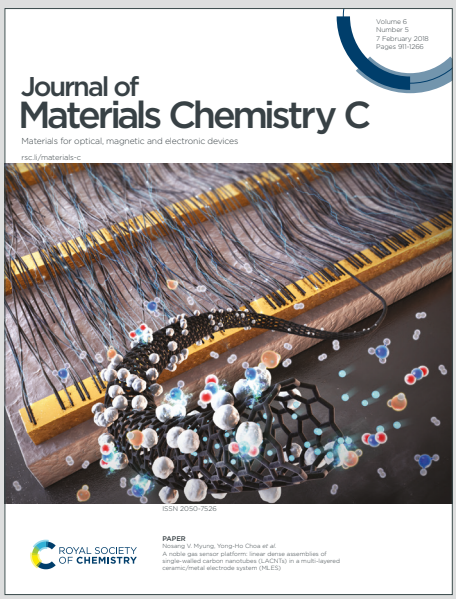

This is an Accepted Manuscript, which has been through the Royal Society of Chemistry peer review process and has been accepted for publication.

Accepted Manuscripts are published online shortly after acceptance, before technical editing, formatting and proof reading. Using this free service, authors can make their results available to the community, in citable form, before we publish the edited article. We will replace this Accepted Manuscript with the edited and formatted Advance Article as soon as it is available.

You can find more information about Accepted Manuscripts in the Information for Authors.

Please note that technical editing may introduce minor changes to the text and/or graphics, which may alter content. The journal's standard Terms & Conditions and the Ethical guidelines still apply. In no event shall the Royal Society of Chemistry be held responsible for any errors or omissions in this Accepted Manuscript or any consequences arising from the use of any information it contains.

ROYAL SOCIETY OF CHEMISTRY

rsc.li/materials-c

View Article Online
DOI: 10.1039/D5TC03779D

Role of the donor on the light-induced degradation of Y6 non-fullerene acceptors in PM6:Y6 blend films

Suraj Prasad, C. Moyses Araujo, Ellen Moons*

Department of Engineering and Physics, Karlstad University, SE-65188 Karlstad, Sweden.

** Corresponding author (e-mail: ellen.moons@kau.se)*

Open Access Article. Published on 23 December 2025. Downloaded on 1/20/2026 8:25:53 AM.
This article is licensed under a Creative Commons Attribution 3.0 Unported Licence.

Journal of Materials Chemistry C Accepted Manuscript

Abstract:

Despite the rapid advancements in the performance of organic solar cells (OSCs), improving their operational lifetime remains a significant challenge. The photodegradation of donor polymer PM6, small molecule non-fullerene acceptor (NFA) Y6, and their blend was investigated under ambient conditions. To photodegrade the spin-coated thin films, samples were exposed to AM 1.5 illumination, as well as UV-filtered and long-wavelength-filtered light. The evolution of their properties with increasing exposure time up to 45 h was monitored using UV-vis absorption, Fourier transform infrared (FTIR), and photoemission spectroscopy. The results demonstrate that neat PM6 films exhibit faster absorbance loss than the neat Y6 films. This is accompanied by the formation of new carbonyl groups on PM6, while only minor indications of photooxidation were observed in degraded Y6 films. The valence band spectra of Y6 remain unchanged upon photodegradation. Interestingly, the photobleaching rate of Y6 in PM6:Y6 blend films was found to be higher than that of neat Y6 films. XPS spectra of C 1s and S 2p confirm photooxidation products formed in PM6 and PM6:Y6 films, evidenced by new oxidized carbonyl C 1s and oxidized sulfur S 2p peaks. Under AM 1.5 illumination, several photooxidation pathways can be active, involving the formation of both superoxide radicals and singlet oxygen species, and their subsequent oxidation reactions with conjugated molecules. Using filtered light conditions, these different degradation pathways could be separated. Upon exposure to long-wavelength-filtered light, which is predominantly absorbed by the Y6 acceptor, the generation of superoxide radicals is significantly suppressed, resulting

View Article Online
DOI: 10.1039/D5TC03779D

in enhanced photostability of the blend compared to illumination with unfiltered light. The remaining photodegradation of the blend components under these illumination conditions can therefore be ascribed to energy transfer from the photosensitizing acceptor, feeding into the singlet oxygen formation. These insights could inspire the design of new donor and acceptor materials with improved photostability by tuning the positions of their singlet and triplet states to minimize the formation of oxygen-mediated reactive species.

Keywords: light-induced degradation, superoxide radicals, singlet oxygen, electron transfer, and energy transfer.

1. Introduction

Organic solar cells (OSCs) are an emerging photovoltaic technology, driven by their unique advantages, such as mechanical flexibility, light-weight, the potential for cost-effective large-area fabrication,[1-3] and their short energy payback time.[4-6] Over the past decade, following the synthesis of non-fullerene acceptors (NFAs)[7,8] and the development of various processing strategies for active layers, OSCs have shown a tremendous improvement in power conversion efficiency (PCE), now exceeding 19% for single junction solar cells.[9-11] However, the operational lifetime of OSCs is limited, which remains a challenge for outdoor use.[12-14] To address the limited lifetime, it is essential to understand the degradation mechanisms of OSCs and their molecular constituents, including the effect of environmental factors, such as light, heat, moisture, and oxygen.[15-17] Light, in particular high-energy photons in the UV spectral range, can independently induce photodegradation of molecular materials,[18,19] and degrade the OSC's performance.[18] In the presence of oxygen and water vapor that diffuse into the active layer of the devices,[20,21] their exposure to light can lead to photooxidation of the donor and acceptor components, but also of the electrodes and interface layers.[19,22] One of the strategies

Open Access Article. Published on 23 December 2025. Downloaded on 1/20/2026 8:25:53 AM.
This article is licensed under a Creative Commons Attribution 3.0 Unported Licence.

Journal of Materials Chemistry C Accepted Manuscript

View Article Online
DOI: 10.1039/D5TC03779D

Open Access Article. Published on 23 December 2025. Downloaded on 1/20/2026 8:25:53 AM.
This article is licensed under a Creative Commons Attribution 3.0 Unported Licence.

Journal of Materials Chemistry C Accepted Manuscript

to avoid this (photo)chemical degradation by air components is to adequately encapsulate the OSCs.[23-25] Heat is another degradation factor that can contribute to changes in the morphology.[26]

It has been established that two types of oxygen-mediated species may contribute to the degradation of performance in fullerene- and NFAs-based OSCs: superoxide radicals (O_2^-) and the reactive singlet oxygen ($^1O_2$) species.[27-29] The superoxide anion can be generated through photoinduced electron transfer from an excited molecular state to a dioxygen molecule in the environment, provided that the excited state has a higher energy than the reduction potential of O_2.[29,30] In contrast, the $^1O_2$ species is formed by energy transfer from the triplet excited state of a molecule (photo-sensitizer) to ground state molecular oxygen. Upon photoexcitation of the blend, one of the components, either the donor or the acceptor, or both, can trigger photochemical reactions, forming oxygen-based radical species, such as hydroxyl or alkylperoxyl radicals, which can further drive the photooxidation of the donor or acceptor.[27] All these factors can significantly impact the stability and lifetime of unencapsulated OSCs in ambient conditions. While encapsulated devices demonstrate substantially longer operational lifetimes, the diffusion of air components through non-ideal encapsulants, particularly through sealants and flexible substrates, remains a significant degradation pathway. To improve the photostability of the active layers/devices, various strategies have been applied, for example, materials design,[23,31] solvent additives,[32] and UV absorbents[33-35]. We and others have previously demonstrated that, relative to fullerene acceptors, most NFAs exhibit superior photostability under ambient air conditions.[19,36,37] In our previous work, we elucidated the influence of molecular structure, in particular the presence of the BDT moiety, on photodegradation by comparing three NFAs: Y5, PYT, and PF5-Y5.[19] The results demonstrate that replacing the BDT moiety in PF5-Y5 with a thiophene unit in PYT significantly improved the acceptor polymer's intrinsic photostability under AM 1.5 illumination in air. Films of the

View Article Online
DOI: 10.1039/D5TC03779D

Open Access Article. Published on 23 December 2025. Downloaded on 1/20/2026 8:25:53 AM.
This article is licensed under a Creative Commons Attribution 3.0 Unported Licence.

Journal of Materials Chemistry C Accepted Manuscript

small molecule acceptor Y5 are also significantly more resistant to photooxidation than the BDT-containing Y5-based copolymer PF5-Y5. Here, we demonstrate that blending the Y-type NFA Y6 with the polymer donor PM6 leads to an accelerated photodegradation of Y6. Wang *et al.* have studied the photodegradation of Y6, blended with three different donor polymers, PTQ10, PM6, and D18, under white light in air.[38] The authors conclude from *in situ* Raman spectroscopy that the twisting of the BDT moiety in PM6 and D18 was the major cause of the photodegradation. In contrast, PTQ10, which does not contain a BDT moiety, exhibited better photostability.[38,39] In a photodegradation study of PM6:Y6 blend films in N_2 atmosphere, Liu *et al.* demonstrated that the photochemical decomposition of Y6 by UV photons is responsible for the degradation of the PM6:Y6 solar cells.[40] The authors concluded from matrix-assisted laser desorption ionization time-of-flight (MALDI-TOF) mass spectrometry that the breaking of the linkage bond between the core and end groups of Y6 was responsible for the photodegradation.[40]

This study aims to elucidate the contributions of the individual components in PM6:Y6 blend films. UV-vis spectra show that the absorbance of neat Y6 films is relatively stable under exposure to AM 1.5 illumination in air, compared to that of neat PM6 films. We also found that in PM6:Y6 blend films, the acceptor Y6 undergoes photodegradation at a faster rate than in neat Y6 films. To understand the contributions of the donor and acceptor to the light-induced degradation of PM6:Y6 blend film, we investigated their wavelength-dependent photodegradation by exposing the samples to filtered AM 1.5 light using 400 nm (LP400) and 665 nm (LP665) long-pass filters. The degradation rates of both donor and acceptor components in the PM6:Y6 blend films were observed to decrease under LP400 and LP665 illumination, consistent with the reduced light intensity. Nevertheless, even after compensating for the decrease in illuminance, the blend films exhibited slower bleaching and formed fewer photooxidation products under LP665 illumination. This is because the donor does not

View Article Online
DOI: 10.1039/D5TC03779D

Open Access Article. Published on 23 December 2025. Downloaded on 1/20/2026 8:25:53 AM.
This article is licensed under a Creative Commons Attribution 3.0 Unported Licence.

Journal of Materials Chemistry C Accepted Manuscript

significantly absorb high-wavelength light, and therefore, the formation of superoxide is hindered under these conditions. This suggests that the remaining photodegradation of donor and acceptor under LP665 illumination is likely due to singlet oxygen formation, via energy transfer from the photosensitizing acceptor. IR spectra of pure PM6 and PM6:Y6 blend films confirm the formation of new carbonyl groups and breaking of the original quinone group, whereas in pure Y6 films, no significant changes were observed, a finding further corroborated by C 1s and S 2p core-level XPS spectra. The results of this study unravel the photooxidation pathways in PM6:Y6 blends under illumination in ambient conditions and provide insights into the importance of the donor and acceptor's energy levels when aiming at materials for OSCs with enhanced photostability.

2. Experimental

2.1 Materials and sample preparation

The donor polymer PM6 was purchased from 1-Material Inc. and the acceptor Y6 from Sigma Aldrich, respectively. The molecular weight (M_w) of Y6 is 1451.93 g/mol, and for PM6 it is 120,000 g/mol with PDI~2.5, respectively. Chloroform was purchased from Sigma Aldrich (anhydrous, 99.8%). Thin films were deposited on glass substrates for UV-vis absorption spectroscopy and atomic force microscopy (AFM), on KBr pellets for FTIR spectroscopy, and on silicon substrates for photoelectron spectroscopy. The glass substrates were cleaned with acetone and 2-propanol for 10 min each, in an ultrasonic bath, and then UV-ozone treated for 10 min. The KBr substrates (diameter 13 mm, Thermo Fisher Scientific, USA) were used as is. The n-type SiO_X/Si (001) substrates were cleaned using a standard RCA procedure, omitting the final hydrofluoric acid etching step. The coating solutions with concentrations of 16 mg/mL in chloroform were stirred overnight at room temperature. Thin films were spin-coated inside a N_2 filled glove box (O_2 < 10 ppm, H_2O < 0.1 ppm) (MB200MOD, MBraun Inert gas-Systeme

View Article Online
DOI: 10.1039/D5TC03779D

Open Access Article. Published on 23 December 2025. Downloaded on 1/20/2026 8:25:53 AM.
This article is licensed under a Creative Commons Attribution 3.0 Unported Licence.

Journal of Materials Chemistry C Accepted Manuscript

GmbH, Germany) at 3000 rpm for 60 seconds (except for PM6 coated at 6000 rpm for 60 sec) and annealed immediately at 100 °C for 10 min. The thin films were degraded by exposing them in air to white light (AM 1.5) from the solar simulator Sol2A (model 94022A, Oriel Instruments) without filter, and with long-pass filters $\lambda > 400$ nm (LP400) and $\lambda > 665$ nm (LP665) placed between the lamp and the sample. By using the LP400 and LP665 filters, the light intensity is reduced from 1000 W/m^2 to ~ 926 W/m^2 and ~ 607 W/m^2, respectively. The exposure was done stepwise on the same sample for the chosen exposure times of 30 min, 2 h, 10 h, 24 h, and 45 h.

2.2 Experimental methods

The UV-vis absorption spectra were collected in transmission mode between 300 and 1000 nm with a Cary 5000 UV-vis-NIR spectrophotometer (Agilent Technologies, USA), equipped with Cary WinUV 6.1 software. For the background measurements, a cleaned glass substrate was used as a reference sample, and its spectrum was subtracted from the measured spectrum of the thin film coated on glass. Fourier-transform infrared (FTIR) spectra of the thin films on KBr platelets were recorded in transmission mode in the wavenumber range 600-4000 cm^{-1} with an INVENIO S spectrometer (Bruker, France) purged with dry air, equipped with OPUS 8.5 software. The sample thickness and morphology were measured with the Nanoscope 8 Multimode AFM (Bruker, France) in tapping mode with AFM tips (RTESPA-300) purchased from Bruker. The thickness of the films was determined by scanning the AFM tip across a scratch made in the film. The film thicknesses for PM6, Y6, and PM6:Y6 were 94 nm, 72 nm, and 94 nm, respectively. The high-resolution X-ray photoelectron spectroscopy (XPS) measurements were carried out at the FlexPES beamline of the MAX IV synchrotron in Lund, Sweden.[41] The experiments used a defocused X-ray beam with a slit size of 5 µm and a Scienta DA-30L (W) electron analyzer, operated at normal emission, with a pass energy of 50 eV. For

View Article Online
DOI: 10.1039/D5TC03779D

Open Access Article. Published on 23 December 2025. Downloaded on 1/20/2026 8:25:53 AM.
This article is licensed under a Creative Commons Attribution 3.0 Unported Licence.

Journal of Materials Chemistry C Accepted Manuscript

the XPS measurements, the different core levels were measured at the same kinetic energy of approximately 60 eV to maintain a consistent information depth. The photon energies used for the F 1s, O 1s, N 1s, C 1s, and S 2p core levels were 750 eV, 590 eV, 465 eV, 350 eV, and 225 eV, respectively. For the VB spectrum and secondary electron cutoff (SECO) measurements, a photon energy of 45 eV was used, and a negative bias of 28.46 V was applied to the sample holder. The system was maintained at an ultra-high vacuum with a base pressure of 3×10^{-10} mbar. The core level spectra were fitted with CasaXPS software,[42] applying a composite peak shape, consisting of 30% Lorentzian and 70% Gaussian components. The sulfur 2p doublet ($2p_{3/2}$ and $2p_{1/2}$) was fitted with a fixed energy separation of 1.18 eV, a consistent 2:1 intensity ratio, and equal full widths at half maximum (FWHM).[43] For quantitative analysis, a Shirley background subtraction method was utilized.[44,45]

3. Results and discussion

3.1 Photobleaching of pristine and blend films

Figure 1 (a, b) shows the chemical structures of the donor polymer PM6 and the NFA Y6, respectively. The optical absorption spectra of PM6 and Y6 films are shown in Figure 1 (c, d). The main absorption bands of PM6 have maxima at 575 nm and 617 nm, corresponding to the A_{0-1} and A_{0-0} transitions, respectively,[46,47] and smaller absorption peaks at 364 nm and 420 nm. The spectrum resembles that of PBDB-T films.[19] Upon illumination to AM 1.5 light in air, the absorbance of the A_{0-1} and A_{0-0} peaks decreases, reaching an absorbance loss of 33% and 42% after 45 h, respectively, as presented in Table 1. The absorbance of the peaks at 364 nm and 420 nm has decreased by 19% and 12% after 45 h of exposure, while the absorbance increases slightly in the 450-500 nm region with increasing exposure time. Also, an increase in absorption tail is observed at 700-800 nm, which could indicate the formation of sub-gap

View Article Online
DOI: 10.1039/D5TC03779D

Open Access Article. Published on 23 December 2025. Downloaded on 1/20/2026 8:25:53 AM.
This article is licensed under a Creative Commons Attribution 3.0 Unported Licence.

Journal of Materials Chemistry C Accepted Manuscript

energy states upon photodegradation.[19,38] An isosbestic point is located at 649 nm, where the absorbance is independent during the photochemical reaction.

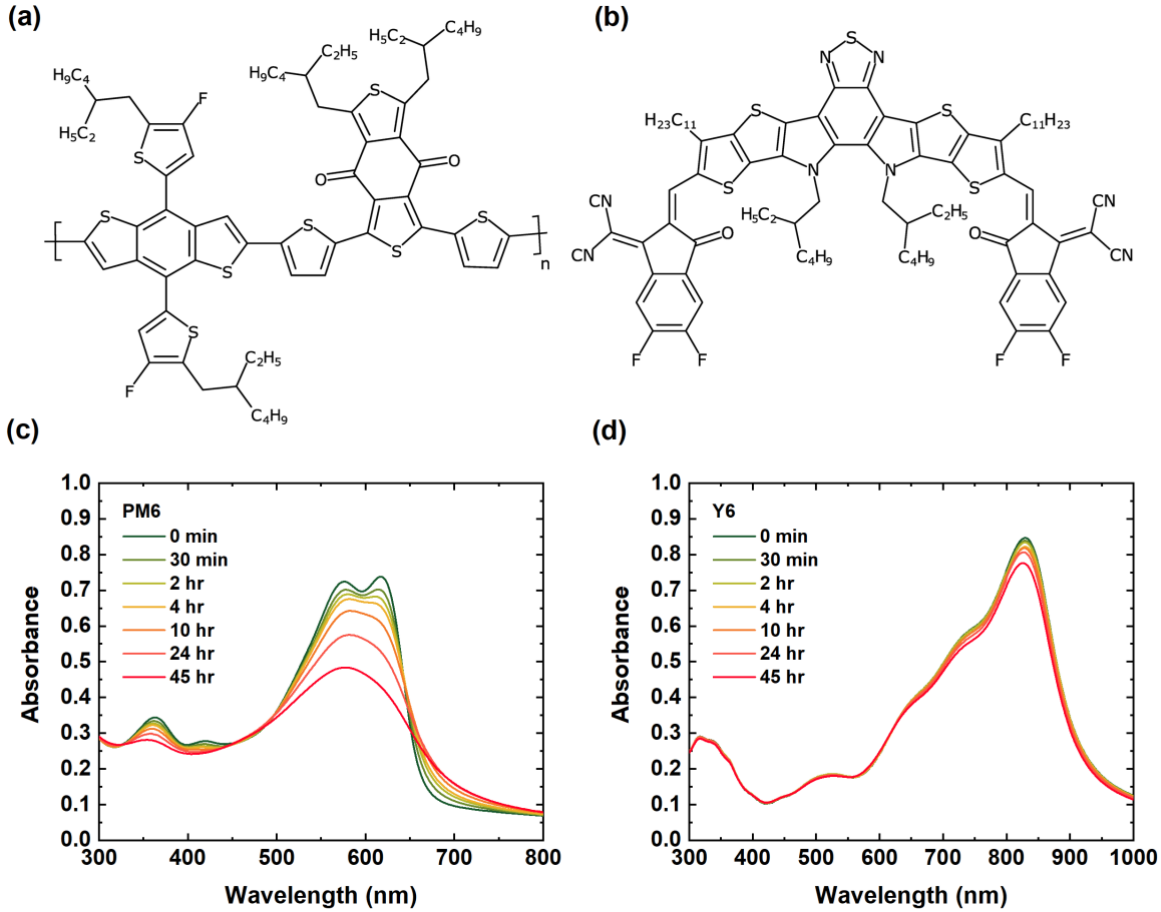

Figure 1: The chemical structures of (a) PM6 and (b) Y6. The optical absorption spectra of spin-coated films of (c) PM6 and (d) Y6, unexposed and exposed in air under AM 1.5 (unfiltered) light for 30 min, 2 h, 4 h, 10 h, 24 h, and 45 h.

For Y6, the intensity of the main absorption peak at 828 nm decreases by 8% upon exposure to AM 1.5 light in air for 45 h, and the shoulder peak at around 735 nm decreases slightly, while the other absorption bands with maxima at shorter wavelengths (317 nm and 520 nm) remain unaffected. From the UV-vis absorption spectra, it can be concluded that the donor PM6 film photobleaches significantly faster than the acceptor Y6 film. Values for the relative absorbance losses after 45 h of exposure are summarized in Table 1 and the evolution of the

View Article Online
DOI: 10.1039/D5TC03779D

Open Access Article. Published on 23 December 2025. Downloaded on 1/20/2026 8:25:53 AM.
This article is licensed under a Creative Commons Attribution 3.0 Unported Licence.

Journal of Materials Chemistry C Accepted Manuscript

normalized absorbance at selected wavelengths, corresponding to the absorption maxima, is summarized in Figure S1. As a subsequent step, the optical absorption spectra of fresh and photodegraded PM6:Y6 (1:1) blend films were recorded and systematically compared with those of the corresponding pristine neat films of PM6 and Y6.

Table 1: The relative change in absorbance of PM6, Y6, and PM6:Y6 blend films at given wavelengths after 45 h of exposure to different illumination conditions, extracted from Figure 1, 2, and Figure S2

Filters	PM6 in neat film (at 617 nm)	PM6 in blend film (at 627 nm)	Y6 in neat film (at 828 nm)	Y6 in blend film (at 814 nm)
No filter	42%	27%	8%	16%
LP 400	25%	19%	4%	9%
LP 665	6%	15%	3%	7%

Figure 2 shows the absorption spectra of fresh and photodegraded PM6:Y6 blend film. The degraded films were continuously exposed in air to AM 1.5 without a filter, with a 400 nm long-pass filter (LP400), and a 665 nm long-pass filter (LP665), before measuring their absorption spectra. The transmission spectra of the LP400 and LP665 filters are shown in Figure S3. In the absorption spectra of the unexposed PM6:Y6 blend (Figure 2a-c), the main absorption peaks are located at 582 nm and 627 nm, primarily from PM6, and at 814 nm, uniquely from Y6. Compared to the pure films, the absorption maxima in the blend film have shifted slightly, to longer wavelengths (by 10 nm) for the 582 and 627 nm peaks (compared to neat PM6), and to shorter wavelengths (by 14 nm) for the 814 nm peak (compared to neat Y6). These shifts may result from donor-acceptor interactions, or differences in molecular packing between the blend and neat films.

View Article Online
DOI: 10.1039/D5TC03779D

Open Access Article. Published on 23 December 2025. Downloaded on 1/20/2026 8:25:53 AM.
This article is licensed under a Creative Commons Attribution 3.0 Unported Licence.

Journal of Materials Chemistry C Accepted Manuscript

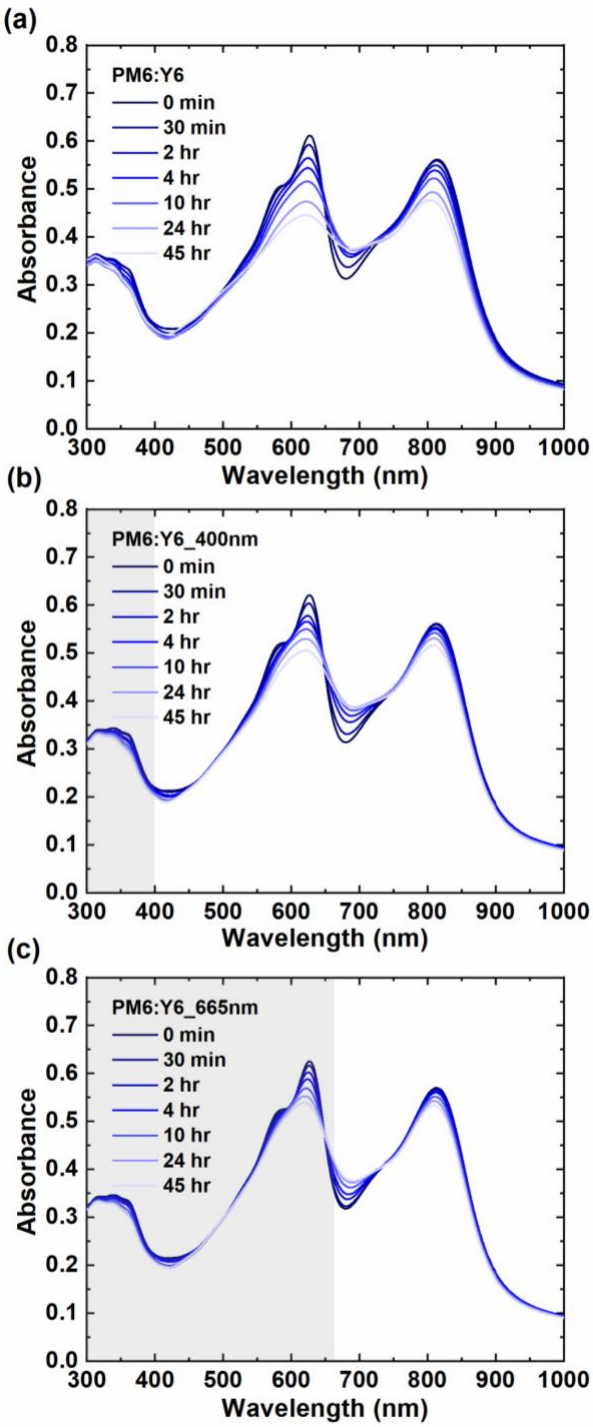

Figure 2: The optical absorption spectra of spin-coated films (a-c) PM6:Y6 (1:1) measured in air before and after photodegradation by exposure for different times (30 min, 2 h, 10 h, 24 h, and 45 h) to AM1.5 light in air without filter (a), with LP400 (b), and with LP665 (c) filters. The grey area indicates the part of the spectrum that is blocked by the filter during the degradation process.

View Article Online
DOI: 10.1039/D5TC03779D

Open Access Article. Published on 23 December 2025. Downloaded on 1/20/2026 8:25:53 AM.
This article is licensed under a Creative Commons Attribution 3.0 Unported Licence.

Journal of Materials Chemistry C Accepted Manuscript

Upon illumination under AM 1.5 light in air, the absorbance at the wavelengths corresponding to the $A_{0\text{-}0}$ and $A_{0\text{-}1}$ bands of PM6 decreases, reaching an absorbance loss after 45 h of 27% and 18%, respectively, as presented in Table 1. The absorbance at 814 nm, originating from Y6 in the blend film, was reduced by 16% after 45 h of exposure. Values for the relative absorbance losses after 45 h of exposure are summarized in Table 1 and the evolution of the normalized absorbance at selected wavelengths, corresponding to the absorption maxima, with exposure time, is summarized in Figure S1. Comparison of the values in Table 1 indicates that the degradation of Y6 is accelerated in the PM6:Y6 blend film relative to the neat Y6 film. It is noted that an increase in absorbance is observed in the wavelength range of 658-722 nm for the blend, similar to that observed in the pure PM6 spectra. This increase may indicate the formation of new species during photodegradation.

3.2 Degradation processes in the blend film

The photodegradation of the donor-acceptor blend film in air can be divided into three different mechanisms: (1) the absorption of photons, including high-energy photons by donor and acceptor, (2) the formation of superoxide radicals (O_2^-) and/or singlet oxygen ($^1O_2$), (3) the reaction of the reactive oxygen species (ROS) with the conjugated molecules.[30,48-51] All three possible degradation pathways can be active under unfiltered light and LP400 filtered light: (1) direct photodegradation, (2) photooxidation via superoxide anion, formed by electron transfer, and (3) photooxidation by singlet oxygen, formed by energy transfer. If an energy level lies above the reduction potential of O_2 (3.75 eV), as illustrated for the donor in Figure 3a, electron transfer from the excited state to molecular oxygen can occur, leading to the formation of a superoxide radical.[29,30] When the excited-state energy of the molecule lies below the reduction potential of O_2, electron transfer to molecular oxygen is hindered, as illustrated in Figure 3a

View Article Online
DOI: 10.1039/D5TC03779D

for Y6. In this case, energy transfer from the acceptor triplet state to ground-state triplet oxygen can occur, generating singlet oxygen (Figure 3b).

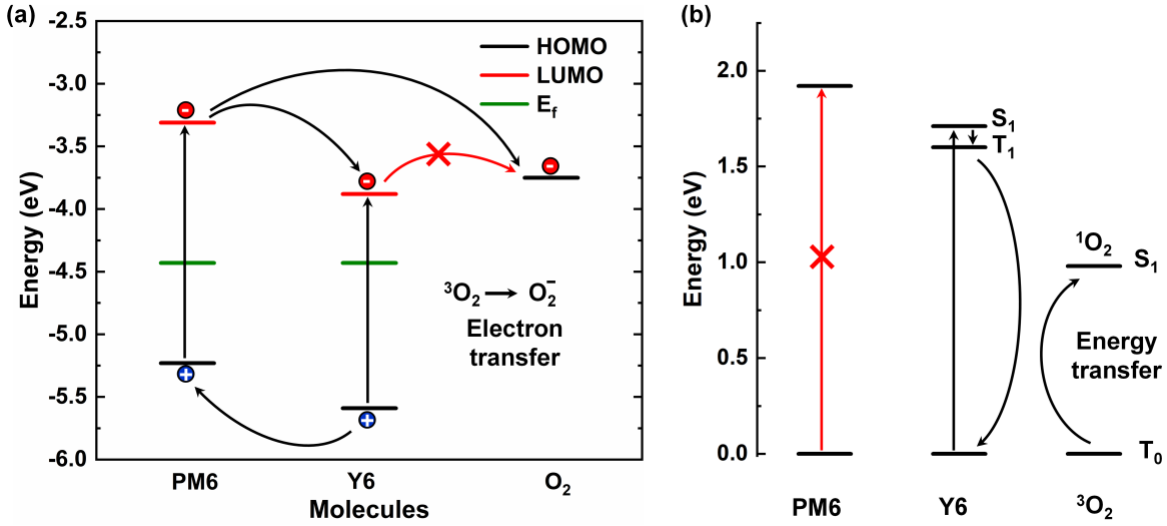

Figure 3: (a) Energy level diagram of the PM6:Y6 blend, illustrating the allowed electron and hole transfer processes and O_2^- (superoxide) generation following the donor excitation under AM 1.5 light and LP400 conditions. The energy level diagram for PM6 and Y6, referenced to the vacuum level, was constructed using the work function and valence band onset values measured by UPS. For the optical band gap of PM6 and Y6 literature values were used.[52] (b) Energy level diagram of the PM6:Y6 blend, illustrating the energy transfer process from the acceptor to O_2, under LP665 illumination, resulting in $^1O_2$ (singlet oxygen) generation.

Figures 3a and 3b illustrate the allowed photophysical processes: electron transfer from the donor LUMO to ground-state oxygen, forming superoxide species, and energy transfer from the acceptor to ground-state oxygen, generating singlet oxygen. Once formed, these reactive species can react with the conjugated molecules PM6 and Y6 in the blend film, resulting in the formation of oxidation products. To investigate the effect of high-energy UV photons, the PM6:Y6 thin film is compared with one exposed to LP400-filtered light, which excludes UV photons. The absorption spectra of PM6:Y6 films under the LP400 filtered light are shown in

Open Access Article. Published on 23 December 2025. Downloaded on 1/20/2026 8:25:53 AM.
This article is licensed under a Creative Commons Attribution 3.0 Unported Licence.

Journal of Materials Chemistry C Accepted Manuscript

View Article Online
DOI: 10.1039/D5TC03779D

Open Access Article. Published on 23 December 2025. Downloaded on 1/20/2026 8:25:53 AM.
This article is licensed under a Creative Commons Attribution 3.0 Unported Licence.

Journal of Materials Chemistry C Accepted Manuscript

Figure 2b. The absorbance of PM6 and Y6 components in the PM6:Y6 blend film decreased by 19% and 9%, respectively, after 45 h of LP400 illumination, as shown in Table 1. Compared to pure component films, these absorption losses in the PM6:Y6 blend film upon illumination with AM 1.5 light filtered with a 400 nm long-pass filter were reduced by a factor of 1.4 and 1.8 for the PM6 and Y6 components, respectively. It is well established that high-energy UV photons can induce photodegradation of conjugated molecules by cleaving the weakest bonds in the molecule.[50,51] Finally, the PM6:Y6 film was exposed to AM 1.5 illumination filtered through a 665 nm long-pass filter (LP665). Under these conditions, light absorption in the long-wavelength region is primarily attributed to Y6, with only a minor contribution from the PM6 absorption tail. In Table 1 and Figure 2c, it is shown that PM6 and Y6 degrade by 15% and 7%, respectively, after exposure to LP665 for 45 h. Compared to unfiltered light, the exposure of the PM6:Y6 blend to LP665 light decreases the absorbance losses by a factor of 1.8 for PM6 and 2.3 for Y6. Notably, the donor PM6 still undergoes approximately 15% degradation after exposure of the PM6:Y6 blend film to LP665 illumination for 45 h. Electron transfer from excited Y6 is prohibited under all illumination conditions, because the LUMO of the Y6 acceptor is lower (deeper) than the reduction potential of oxygen (Figure 3a). Additionally, energy transfer from the excited state of Y6 to ground-state oxygen can occur, leading to the generation of singlet oxygen. This suggests that singlet oxygen is responsible for the degradation of both the acceptor and the donor under these illumination conditions, as illustrated in Figure 3b. To further investigate light-induced degradation, we quantified the absorbance losses of neat PM6, neat Y6, and a PM6:Y6 blend film after 45 h of LP665-filtered illumination. The neat PM6 and Y6 films exhibited absorbance decreases of 6% and 3%, respectively. In contrast, in the PM6:Y6 blend, the PM6 and Y6 components showed larger losses of 15% and 7%, respectively. These results indicate that both materials are less photostable in the blend than in their neat films, and that PM6 degrades more rapidly than Y6

View Article Online
DOI: 10.1039/D5TC03779D

Open Access Article. Published on 23 December 2025. Downloaded on 1/20/2026 8:25:53 AM.
This article is licensed under a Creative Commons Attribution 3.0 Unported Licence.

Journal of Materials Chemistry C Accepted Manuscript

within the blend. The accelerated degradation observed in the blend is likely associated with energy transfer processes. Notably, the degradation of Y6 increases from 3% in the neat film to 7% in the blend under LP665-filtered light, indicating that the presence of the donor significantly accelerates the degradation rate, even under illumination conditions where the PM6 donor exhibits only minimal absorbance.

3.3 Analysis of photodegradation products

To investigate the photochemical degradation products upon exposure to light (AM 1.5), infrared spectra were recorded of films of PM6, Y6, and PM6:Y6 (1:1), spin-coated on KBr substrates, in transmission mode. The samples were processed and photodegraded under the same conditions as those used for the UV-vis absorption spectroscopy.

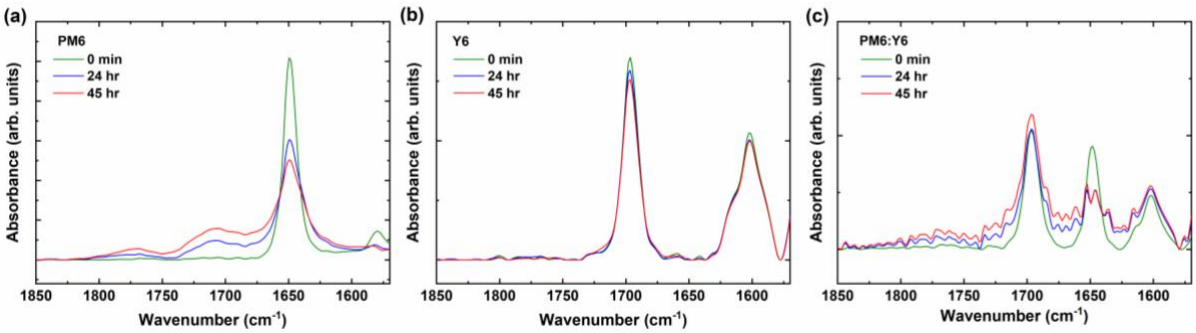

Figure 4: FTIR spectra measured in transmission mode, of spin-coated films of pristine (a) PM6, (b) Y6, and (c) PM6:Y6 (1:1) on KBr, unexposed and exposed under white light (AM 1.5) for 45 h. The wide range spectra are shown in Figure S4.

Figure 4 shows the FTIR spectra of PM6 (a), Y6 (b), and PM6:Y6 (c) films in the extended carbonyl region, ranging from 1850 cm^{-1} to 1570 cm^{-1}, before and after exposure to unfiltered white light (AM 1.5) in air for 45 h. The wide range FTIR spectra are shown in Figure S4. The peak positions and their corresponding assignments are summarized in Tables S1 and S2. For PM6, the most significant changes after 45 h exposure are seen in the carbonyl region of the

View Article Online
DOI: 10.1039/D5TC03779D

Open Access Article. Published on 23 December 2025. Downloaded on 1/20/2026 8:25:53 AM.
This article is licensed under a Creative Commons Attribution 3.0 Unported Licence.

Journal of Materials Chemistry C Accepted Manuscript

IR spectrum (Figure 4a), namely the intensity drop of the sharp peak at 1649 cm^{-1} corresponding to the C=O stretch in the quinone group, accompanied by the development of two new peaks with maxima at 1709 cm^{-1} and 1770 cm^{-1}.[53,54] The new peak at 1709 cm^{-1} can be assigned to the ester group, and the peak at 1770 cm^{-1} can be assigned to the anhydride group.[55] A similar growth of a peak at 1770 cm^{-1} has been observed in photo-oxidized PBDB-T and $PC_{60}BM$.[19,56,57] We also note that the peak at 1709 cm^{-1} grows 64% faster than the 1770 cm^{-1} peak. Smaller changes are also observed (see Figure S4), such as a decrease in absorption intensity of the four sharp peaks between 1400 and 1100 cm^{-1}, corresponding to C-H rocking and scissoring modes.[19,38,55,58] In addition, the peak intensities at ~1177 cm^{-1} and ~1550 cm^{-1} remain unchanged. The results indicate that PM6 undergoes photo-oxidation, affecting both the quinone group, the side chains, and the backbone of the molecule. These findings contrast with the report by Wang *et al.* indicating that photodegradation of PM6 under white-light exposure in air induces twisting of the BDT-T unit.[38]

Figure 4b shows the carbonyl region of the IR spectra of Y6, characterized by two strong peaks, one at 1697 cm^{-1} that corresponds to the symmetric C=O stretch vibration of the terminal groups from the five-membered carbon ring and a peak at 1600 cm^{-1}, which corresponds to the C=N stretch of the fused benzothiadiazole aromatic core.[53,55,59] In Figure S4, we also identify the corresponding peaks for C≡N stretch vibration at 2216 cm^{-1} and 1535 cm^{-1} as malononitrile moieties dominated by C-C mode,[60] while the C=C stretch mode of thiophene is found at 1506 cm^{-1} and from the conjugate plane at 1426 cm^{-1}.[55] Upon photooxidation for 45 h, the Y6 films showed a minor decrease in the intensity of the peaks at 1535 cm^{-1}, 1426 cm^{-1}, 1290 cm^{-1}, 1253 cm^{-1}, 1230 cm^{-1}, and 1150 cm^{-1}. This indicates that the Y6 acceptor is less susceptible to degradation than the PM6 donor, in agreement with the UV-vis absorption spectra. The FTIR spectra of PM6:Y6 (1:1) are shown in Figure 4c. The peak at 1649 cm^{-1} that was identified above as the C=O stretch in PM6 decreases rapidly upon photodegradation, as it did for neat

View Article Online
DOI: 10.1039/D5TC03779D

Open Access Article. Published on 23 December 2025. Downloaded on 1/20/2026 8:25:53 AM.
This article is licensed under a Creative Commons Attribution 3.0 Unported Licence.

Journal of Materials Chemistry C Accepted Manuscript

PM6 films. A new shoulder appears at 1722 cm^{-1} and 1770 cm^{-1} after exposure for 45 h, possibly indicating the formation of an ester and anhydride group. The peak intensity at 1697 cm^{-1}, which was assigned to the C=O stretch and the peak at 1600 cm^{-1} for the C=N stretch of Y6, remains almost unchanged. The strong peaks originating from Y6 at 2216 cm^{-1}, 1535 cm^{-1}, 1426 cm^{-1}, and 1290 cm^{-1} decrease, indicating that C≡N, malononitrile moieties, and C=C are also affected (see Figure S4). The peaks at 1230 cm^{-1} and 1254 cm^{-1} show a smaller decrease in intensity compared to pure Y6 films. Interestingly, the intensities of the peaks at 1506 cm^{-1} and 1100 cm^{-1} remain unchanged, which was not the case for pure Y6 films. The peak positions of PM6:Y6 films can be compared with those in the IR spectra of the pure PM6 and Y6 films in Figure S4. To further investigate the effect of light-induced degradation, the IR spectra of PM6:Y6 blend films exposed to LP400 and LP665 filtered light were measured and compared to the IR spectra of samples exposed to AM1.5 light, as shown in Figure S5 (a, b, c). As expected from the UV-vis absorption spectra, using the 400 nm and 665 nm long pass filter, the peak intensities of the strong IR peaks at 1149 cm^{-1}, 1230 cm^{-1}, 1290 cm^{-1}, 1426 cm^{-1}, and 1535 cm^{-1} were suppressed after 45 hr of photodegradation. The emergence of new shoulder peaks at 1722 cm^{-1} and 1770 cm^{-1} after 45 h of exposure indicates the formation of ester and anhydride groups under both LP400 and LP665 filtered light, which were also suppressed. The peak at 1649 cm^{-1} is further suppressed under the LP665 condition compared to the no filter condition.

The AFM height images of pure PM6, pure Y6, and PM6:Y6 blend at 0 min and 45 h of exposure under simulated sunlight in ambient conditions are shown in Figure S6. The height image of the 0 min PM6 and PM6:Y6 surface shows a fiber-like structure with surface roughness values of 0.98 nm and 0.77 nm, respectively. However, the Y6 films exhibit interconnected domains with a surface roughness of 1.27 nm. Upon exposure to light for 45 h in ambient conditions, the PM6, Y6, and PM6:Y6 films show a minor decrease in roughness

View Article Online
DOI: 10.1039/D5TC03779D

Open Access Article. Published on 23 December 2025. Downloaded on 1/20/2026 8:25:53 AM.
This article is licensed under a Creative Commons Attribution 3.0 Unported Licence.

Journal of Materials Chemistry C Accepted Manuscript

with 0.96 nm, 1.24 nm, and 0.71 nm. From the AFM images, it can be concluded that after 45 h of photodegradation, the surface morphology of the pure PM6, pure Y6, and blend PM6:Y6 films remains unchanged.

To investigate the effects of photodegradation on the surfaces of PM6, Y6, and PM6:Y6 blend films, high-resolution XPS core-level spectra (C 1s, S 2p, O 1s, F 1s, and N 1s) and wide survey spectra were collected for both fresh (0 h) and photodegraded (45 h) samples. The survey spectrum of PM6, Y6, and PM6:Y6 is shown in Figure S7.

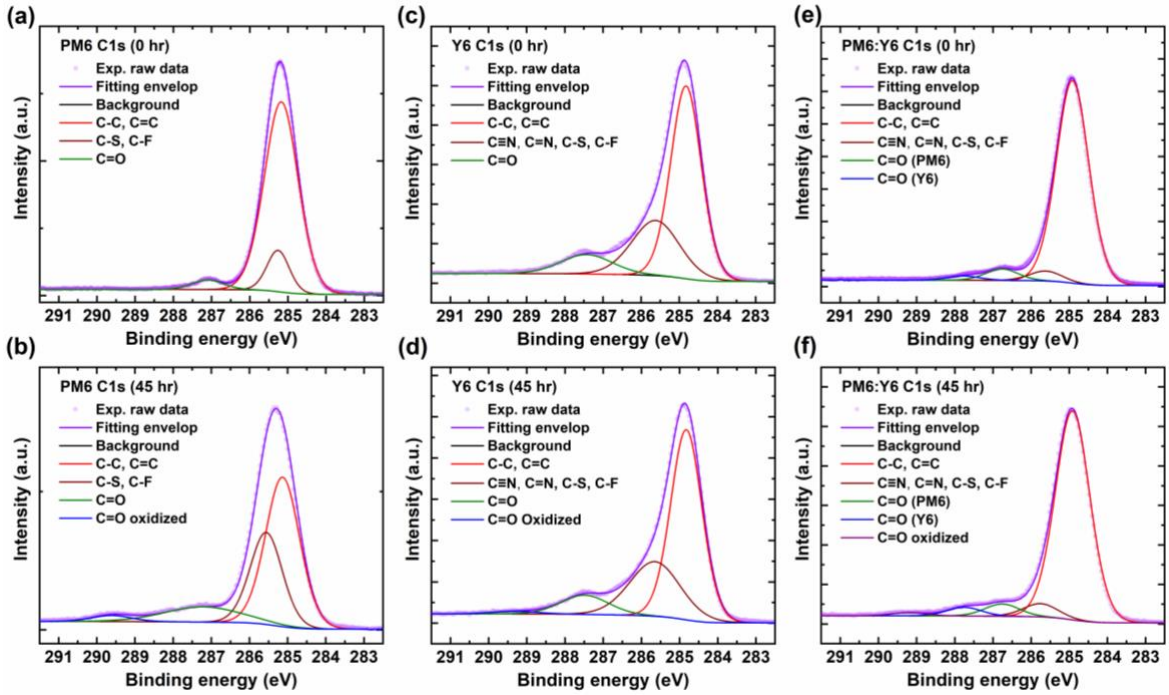

Figure 5: High-resolution XPS core level C 1s spectra of PM6 (left), Y6 (middle), and the PM6:Y6 blend (right) films. Spectra are presented for fresh samples (0 h) and after 45 h of degradation under AM 1.5 illumination in air, as indicated in the legends.

Figure 5 shows the core-level spectra of C 1s for the fresh (0 h) and degraded (45 h) samples of PM6, Y6, and PM6:Y6 blend films. In the C 1s spectra of PM6 at 0 h, presented in Figure 5a, the main peak at 285.17 eV corresponds to the C-C and C=C bonds of the aromatic rings and alkyl side chains, and the peak at 285.26 eV contains contributions from C-S and C-F

View Article Online
DOI: 10.1039/D5TC03779D

Open Access Article. Published on 23 December 2025. Downloaded on 1/20/2026 8:25:53 AM.
This article is licensed under a Creative Commons Attribution 3.0 Unported Licence.

Journal of Materials Chemistry C Accepted Manuscript

bonds, while the 287.10 eV component represents the carbonyl of the quinone group. After 45 h of exposure to AM 1.5 light (Figure 5b), the intensity of the main component at 285.17 eV decreases (see Figure S8a), and a new peak appears at a higher binding energy of 289.61 eV. The peak at 285.26 eV, corresponding to C-S and C-F groups, grows and shifts towards higher binding energy at 285.54 eV. A decrease in the intensity of the main peak at 285.17 eV is observed, accompanied by a shift to a higher binding energy at 285.54 eV. The new peak at the higher binding energy of 289.61 eV is assigned to oxidized carbon after photooxidation. The FTIR spectra of PM6 support the formation of new carbonyls. Figure 5c shows the C 1s spectra of Y6 for the fresh sample (0 h). The main peak at 284.82 eV is assigned to C-C and C=C, originating from the aromatic rings and alkyl side chains. The peak at 285.62 eV corresponds to contributions from C-S, C-F, C=N, and C≡N groups, and the 287.43 eV component corresponds to the carbonyl from the terminal groups. The main peak at 284.82 eV decreases more slowly upon photodegradation compared to PM6 (see Figure S8d), and a small new contribution starts to appear at 289.30 eV, as shown in Figure 5d, indicating the formation of new carbonyl groups upon photooxidation. The component at 285.62 eV, corresponding to the mixture of C-S, C-F, C=N, and C≡N bonds, shows an insignificant shift to 285.65 eV. Similarly, the peak at 287.43 eV, attributed to the carbonyl group, shifts insignificantly to 287.49 eV. The core-level C 1s spectra indicate that the Y6 acceptor is relatively more stable than PM6, which is consistent with the observations from the UV-vis and FTIR spectra following photooxidation. Figure 5e shows the C 1s spectra of the PM6:Y6 blend film. The main peak at 284.92 eV corresponds to C-C and C=C bonds of both molecules, as observed in the pristine films. The peak at 285.62 eV corresponds to the mixture of peaks from C-S, C-F, C=N, and C≡N bonds. As expected, in the PM6:Y6 blend, the components at 286.77 eV and 287.77 eV correspond to the carbonyl groups from PM6 and Y6, respectively. After 45 h of exposure to AM 1.5 light (Figure 5f), the main peak at 284.92 eV decreases (see Figure S8g),

View Article Online
DOI: 10.1039/D5TC03779D

Open Access Article. Published on 23 December 2025. Downloaded on 1/20/2026 8:25:53 AM.
This article is licensed under a Creative Commons Attribution 3.0 Unported Licence.

Journal of Materials Chemistry C Accepted Manuscript

while a new peak emerges at a higher binding energy of 289.20 eV. Both the carbonyl peaks from the PM6 and Y6 peaks show a minor shift to higher binding energies at 286.77 eV and 287.77 eV, respectively, upon photooxidation. The O 1s spectra of the PM6, Y6, and PM6:Y6 are shown in Figure S8 (c, f, i). The increase in O 1s peak intensity confirms the addition of oxygen upon photooxidation. Moreover, the addition of oxygen is more pronounced in the PM6 samples compared to Y6 and the PM6:Y6 blend. The S 2p core level spectra for the PM6, Y6, and PM6:Y6 are shown in Figure S9. After 45 h of degradation, new peaks appear at higher binding energies, indicating the formation of oxidized sulfur species (SOx). For completeness, the F 1s core level spectra for PM6, Y6, and the PM6:Y6 blend at 0 h and after 45 h of photooxidation are shown in Figure S10 (a, b, d). After 45 h of exposure, the F 1s spectra of PM6 exhibit only minor changes, indicating the F 1s are only slightly affected upon photodegradation. Moreover, the F 1s spectra of both the Y6 acceptor and the PM6:Y6 blend remain essentially unchanged. Neither the N 1s core level spectra of Y6 nor the ones of PM6:Y6 blend show any significant changes after photooxidation, as presented in Figure S10 (c,e). These results suggest that the F 1s and N 1s core levels remain unaffected by the photodegradation process.

The effect on the frontier energy levels and the work function, induced by photodegradation of PM6, Y6, and the PM6:Y6 blend films, is investigated by the valence band (VB) and SECO spectra shown in Figure 6. Figure 6a shows the VB spectrum of a fresh and degraded (45 h) PM6 film. The valence band onset for the fresh PM6 film is estimated at 0.80 eV with respect to the Fermi level, E_F. After 45 h of degradation, the valence band decreases to 0.78 eV w.r.t. the Fermi level, and the valence band onset is difficult to determine from the UPS spectrum. Also, the valence band spectra of Y6 (Figure 6b) show a valence band onset decrease from 1.16 eV to 0.95 eV w.r.t E_F upon 45 h of photodegradation. It is noteworthy that the shape of the density of states (DOS) for Y6 remains unchanged.

View Article Online
DOI: 10.1039/D5TC03779D

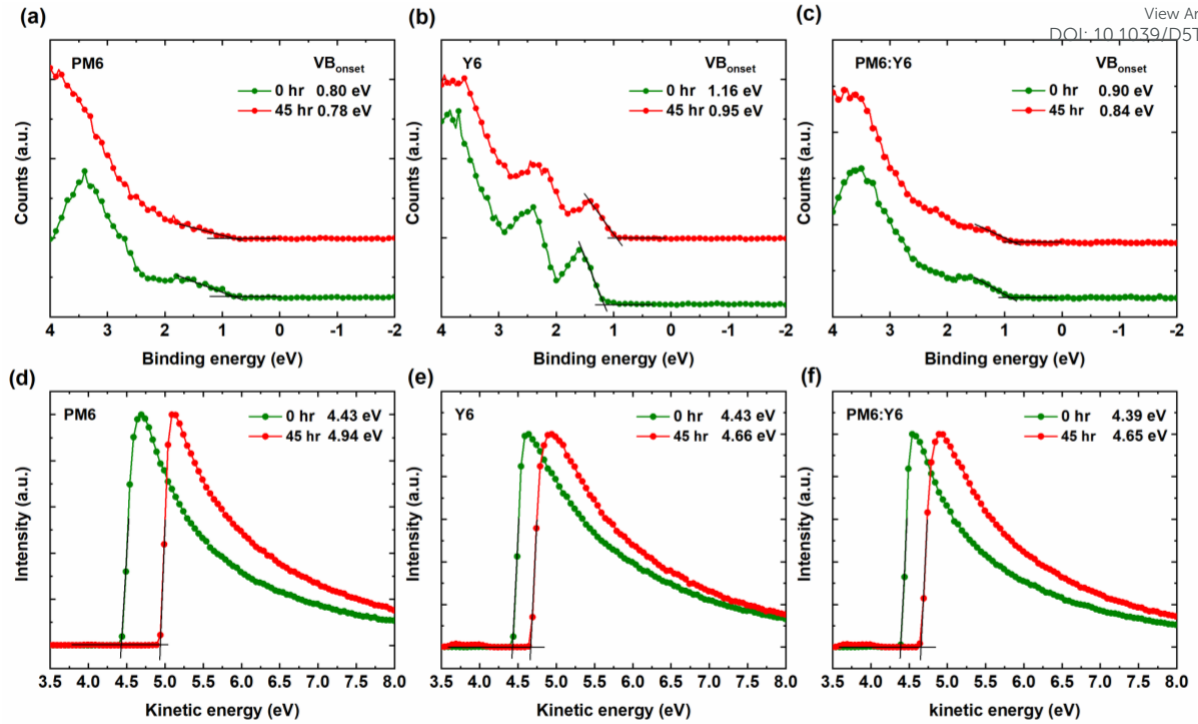

Figure 6: Valence band spectra of (a) PM6, (b) Y6, and (c) PM6:Y6 blend films, along with the secondary electron cutoff (SECO) spectra of (d) PM6, (e) Y6, and (f) PM6:Y6. All spectra are shown for fresh samples (0 h) and after 45 h of degradation under AM 1.5 illumination in air. VB spectra of degraded films are intentionally offset on the y-axis for clarity. The VB onset and work function values are given in the VB spectra and SECO spectra, respectively.

For the PM6:Y6 blend, the initial valence band onset of 0.90 eV decreases slightly to 0.84 eV following 45 h of degradation. The DOS of the blend is dominated by contributions from PM6.[21,61] From the secondary electron cutoff (SECO) spectra, seen in Figures 6d-f, the work function values of PM6, Y6, and the PM6:Y6 blend films were determined for fresh (0 h) and degraded (45 h) samples. Upon photodegradation, the work function of PM6 increases by 0.51 eV from 4.43 eV to 4.94 eV, while that of Y6 increases by 0.23 eV, from 4.43 eV to 4.66 eV. Similarly, the PM6:Y6 blend exhibits a work function increase of 0.26 eV from 4.39 eV to 4.65 eV. The increase in the work functions of PM6, Y6, and PM6:Y6 films can be related to chemical modifications upon photodegradation.[21] These results conclude that

Open Access Article. Published on 23 December 2025. Downloaded on 1/20/2026 8:25:53 AM.
This article is licensed under a Creative Commons Attribution 3.0 Unported Licence.

Journal of Materials Chemistry C Accepted Manuscript

View Article Online
DOI: 10.1039/D5TC03779D

Open Access Article. Published on 23 December 2025. Downloaded on 1/20/2026 8:25:53 AM.
This article is licensed under a Creative Commons Attribution 3.0 Unported Licence.

Journal of Materials Chemistry C Accepted Manuscript

photodegradation induces distinct modifications in the frontier electronic structure across the donor, acceptor, and their blend.

4. Conclusions

We have studied the photodegradation of donor polymer PM6 and the small molecule acceptor Y6, and their blend PM6:Y6 in air under different illumination conditions. The UV-vis absorption spectra show that PM6 films photobleach significantly faster than Y6 films when exposed to AM1.5 light. Notably, the photodegradation of Y6 is accelerated in PM6:Y6 blend films compared to neat Y6 films. To differentiate the degradation pathways associated with reactive oxygen species, the PM6:Y6 blend film was additionally exposed to UV-filtered AM 1.5 light (LP400) and long-wavelength illumination (LP665). Exposure to filtered light results in slower degradation of the blend components compared to unfiltered light. When the blends are exposed to long-wavelength light (LP665), electron transfer is suppressed, thereby preventing the formation of superoxide radicals. The IR spectra of pure PM6 and PM6:Y6 blend films show the formation of new oxidized carbonyl and the breaking of the original quinone group upon photodegradation. Moreover, the C 1s and S 2p XPS spectra confirm the formation of the oxidized carbonyl and additionally oxidized sulfur at the surface of PM6, Y6, and PM6:Y6 films. After 45 h of photodegradation, shifts of 0.02 eV, 0.21 eV, and 0.06 eV on the valence band onset towards the Fermi level for PM6, Y6, and PM6:Y6 samples after exposure. The work function increases after degradation, which could indicate chemical modifications across all samples. This work could inspire the design of new donor and acceptor materials by tuning their singlet and triplet states to prevent photodegradation caused by oxygen-mediated species.

View Article Online
DOI: 10.1039/D5TC03779D

Open Access Article. Published on 23 December 2025. Downloaded on 1/20/2026 8:25:53 AM.
This article is licensed under a Creative Commons Attribution 3.0 Unported Licence.

Journal of Materials Chemistry C Accepted Manuscript

Authors contributions

SP prepared all the samples, conducted the degradation experiments, measured the UV-vis absorption spectra, FTIR spectra, and AFM images, and drafted the first version of the manuscript. SP and EM conducted XPS, VB, and SECO measurements with the help of other co-workers acknowledged. EM and MA supervised the work, contributed to the data analysis and interpretation of the results, and assisted in writing the manuscript. All authors contributed to the final version of the manuscript.

Conflict of interest

The authors have no conflicts of interest.

Data availability

The data supporting this article have been included as part of the supplementary information (SI).

Acknowledgments

The authors would like to thank Dr. Hanmin Zhang, Dr. Cleber F. N. Marchiori, Dr. Leif K. E. Ericsson, Dr. Saurabh Pareek, and Shahna Mysin Kadakkotteeri for their help with XPS and UPS measurements at the MAX IV synchrotron. The authors would also like to thank the beamline scientists, Dr. Alexei Preobrajenski, Dr. Alexander Generalov, and Dr. Stephan Appelfeller, for their assistance with the synchrotron measurements. We acknowledge the MAX IV Laboratory for beamtime on the FlexPES beamline under proposal 20241616. Research conducted at MAX IV, a Swedish national user facility, is supported by Vetenskapsrådet (Swedish Research Council, VR) under contract 2018-07152, Vinnova (Swedish Governmental Agency for Innovation Systems) under contract 2018-04969, and

Formas under contract 2019-02496. We acknowledge funding through the PRISMAS program from the European Union's COFUND action, within the European Commission MSCA framework (Grant agreement ID: 101081419). EM acknowledges the Swedish Energy Agency (contract 48598-1) for financial support of the project. The Knut and Alice Wallenberg Foundation (grant number 2016.0059) is acknowledged for financial support for the research equipment used in the project.

View Article Online
DOI: 10.1039/D5TC03779D

Open Access Article. Published on 23 December 2025. Downloaded on 1/20/2026 8:25:53 AM.
This article is licensed under a Creative Commons Attribution 3.0 Unported Licence.

Journal of Materials Chemistry C Accepted Manuscript

References

1 Y. Li, G. Xu, C. Cui & Y. Li. Flexible and Semitransparent Organic Solar Cells. *Advanced Energy Materials* **8**, 1701791 (2018).

2 L. Sun, K. Fukuda & T. Someya. Recent progress in solution-processed flexible organic photovoltaics. *npj Flexible Electronics* **6**, 89 (2022).

3 F. Yang, Y. Huang, Y. Li & Y. Li. Large-area flexible organic solar cells. *npj Flexible Electronics* **5**, 30 (2021).

4 R. García-Valverde, J. A. Cherni & A. Urbina. Life cycle analysis of organic photovoltaic technologies. *Progress in Photovoltaics: Research and Applications* **18**, 535-558 (2010).

5 S. Lizin, S. Van Passel, E. De Schepper, W. Maes, L. Lutsen, J. Manca & D. Vanderzande. Life cycle analyses of organic photovoltaics: a review. *Energy & Environmental Science* **6**, 3136-3149 (2013).

6 D. Yue, P. Khatav, F. You & S. B. Darling. Deciphering the uncertainties in life cycle energy and environmental analysis of organic photovoltaics. *Energy & Environmental Science* **5**, 9163-9172 (2012).

7 D. Luo, W. Jang, D. D. Babu, M. S. Kim, D. H. Wang & A. K. K. Kyaw. Recent progress in organic solar cells based on non-fullerene acceptors: materials to devices. *Journal of Materials Chemistry A* **10**, 3255-3295 (2022).

8 N. Ahmad, J. Yuan & Y. Zou. One more step towards better stability of non-fullerene organic solar cells: advances, challenges, future perspectives, and the Era of artificial intelligence. *Energy & Environmental Science* **18**, 5093-5158 (2025).

9 Y. Zhang, W. Deng, C. E. Petoukhoff, X. Xia, Y. Lang, H. Xia, H. Tang, H. T. Chandran, S. Mahadevan, K. Liu, P. W. K. Fong, Y. Luo, J. Wu, S.-W. Tsang, F. Laquai, H. Wu, X. Lu, Y. Yang & G. Li. Achieving 19.4% organic solar cell via an in

View Article Online
DOI: 10.1039/D5TC03779D

Open Access Article. Published on 23 December 2025. Downloaded on 1/20/2026 8:25:53 AM.
This article is licensed under a Creative Commons Attribution 3.0 Unported Licence.

Journal of Materials Chemistry C Accepted Manuscript

517 situ formation of p-i-n structure with built-in interpenetrating network. *Joule* **8**, 509-
518 526 (2024).
519 10 D. Meng, R. Zheng, Y. Zhao, E. Zhang, L. Dou & Y. Yang. Near-Infrared Materials:
520 The Turning Point of Organic Photovoltaics. *Advanced Materials* **34**, 2107330
521 (2022).
522 11 Z. Ling, J. Wu, J. P. Jurado, C. E. Petoukhoff, S. Y. Jeong, D. Naphade, M. Babics,
523 X. Chang, H. Faber, S. Doukas, E. Lidorikis, M. I. Nugraha, M. He, M. Alqurashi, Y.
524 Lin, X. Sun, H. Hu, H. Y. Woo, S. De Wolf, L. Tsetseris, F. Laquai, D. Yu, E. Wang
525 & T. D. Anthopoulos. 20.5 % efficient ternary organic photovoltaics using an
526 asymmetric small-molecular acceptor to manipulate intermolecular packing and
527 reduce energy losses. *Materials Science and Engineering: R: Reports* **163**, 100922
528 (2025).
529 12 J. Han, H. Xu, S. H. K. Paleti, A. Sharma & D. Baran. Understanding photochemical
530 degradation mechanisms in photoactive layer materials for organic solar cells.
531 *Chemical Society Reviews* **53**, 7426-7454 (2024).
532 13 M. Riede, D. Spoltore & K. Leo. Organic Solar Cells—The Path to Commercial
533 Success. *Advanced Energy Materials* **11**, 2002653 (2021).
534 14 B. Azzopardi, C. J. M. Emmott, A. Urbina, F. C. Krebs, J. Mutale & J. Nelson.
535 Economic assessment of solar electricity production from organic-based photovoltaic
536 modules in a domestic environment. *Energy & Environmental Science* **4**, 3741-3753
537 (2011).
538 15 L. Duan & A. Uddin. Progress in Stability of Organic Solar Cells. *Advanced Science*
539 **7**, 1903259 (2020).
540 16 Y. Li, T. Li & Y. Lin. Stability: next focus in organic solar cells based on non-
541 fullerene acceptors. *Materials Chemistry Frontiers* **5**, 2907-2930 (2021).
542 17 P. Cheng & X. Zhan. Stability of organic solar cells: challenges and strategies.
543 *Chemical Society Reviews* **45**, 2544-2582 (2016).
544 18 P. Weitz, J. Wortmann, C. Liu, T.-J. Wen, C.-Z. Li, T. Heumüller & C. J. Brabec.
545 Photodegradation of Organic Solar Cells under Visible Light and the Crucial
546 Influence of Its Spectral Composition. *ACS Applied Materials & Interfaces* **16**,
547 36667-36677 (2024).
548 19 S. Prasad, Z. Genene, C. F. N. Marchiori, S. Singh, L. K. E. Ericsson, E. Wang, C. M.
549 Araujo & E. Moons. Effect of molecular structure on the photochemical stability of
550 acceptor and donor polymers used in organic solar cells. *Materials Advances* (2024).

View Article Online
DOI: 10.1039/D5TC03779D

Open Access Article. Published on 23 December 2025. Downloaded on 1/20/2026 8:25:53 AM.
This article is licensed under a Creative Commons Attribution 3.0 Unported Licence.

Journal of Materials Chemistry C Accepted Manuscript

20 M. Hermenau, M. Riede, K. Leo, S. A. Gevorgyan, F. C. Krebs & K. Norrman. Water and oxygen induced degradation of small molecule organic solar cells. *Solar Energy Materials and Solar Cells* **95**, 1268-1277 (2011).

21 Q. Zhang, Y. Chen, X. Liu & M. Fahlman. In situ near-ambient pressure X-ray photoelectron spectroscopy reveals the effects of water, oxygen and light on the stability of PM6:Y6 photoactive layers. *Journal of Materials Chemistry C* **11**, 3112-3118 (2023).

22 Z.-X. Liu, Z.-P. Yu, Z. Shen, C. He, T.-K. Lau, Z. Chen, H. Zhu, X. Lu, Z. Xie, H. Chen & C.-Z. Li. Molecular insights of exceptionally photostable electron acceptors for organic photovoltaics. *Nature Communications* **12**, 3049 (2021).

23 A. J. Clarke, J. Luke, R. Meitzner, J. Wu, Y. Wang, H. K. H. Lee, E. M. Speller, H. Bristow, H. Cha, M. J. Newman, K. Hooper, A. Evans, F. Gao, H. Hoppe, I. McCulloch, U. S. Schubert, T. M. Watson, J. R. Durrant, W. C. Tsoi, J.-S. Kim & Z. Li. Non-fullerene acceptor photostability and its impact on organic solar cell lifetime. *Cell Reports Physical Science* **2**, 100498 (2021).

24 P. Jiang, L. Hu, L. Sun, Z. a. Li, H. Han & Y. Zhou. On the interface reactions and stability of nonfullerene organic solar cells. *Chemical Science* **13**, 4714-4739 (2022).

25 Y. Jiang, L. Sun, F. Jiang, C. Xie, L. Hu, X. Dong, F. Qin, T. Liu, L. Hu, X. Jiang & Y. Zhou. Photocatalytic effect of ZnO on the stability of nonfullerene acceptors and its mitigation by SnO2 for nonfullerene organic solar cells. *Materials Horizons* **6**, 1438-1443 (2019).

26 H. Zhao, N. Prine, S. Kundu, G. Ma & X. Gu. Effect of Thermal Stress on Morphology in High-Performance Organic Photovoltaic Blends. *JACS Au* **4**, 4334-4344 (2024).

27 A. Rivaton, A. Tournebize, J. Gaume, P.-O. Bussière, J.-L. Gardette & S. Therias. Photostability of organic materials used in polymer solar cells. *Polymer International* **63**, 1335-1345 (2014).

28 M. Jørgensen, K. Norrman & F. C. Krebs. Stability/degradation of polymer solar cells. *Solar Energy Materials and Solar Cells* **92**, 686-714 (2008).

29 E. M. Speller, A. J. Clarke, N. Aristidou, M. F. Wyatt, L. Francàs, G. Fish, H. Cha, H. K. H. Lee, J. Luke, A. Wadsworth, A. D. Evans, I. McCulloch, J.-S. Kim, S. A. Haque, J. R. Durrant, S. D. Dimitrov, W. C. Tsoi & Z. Li. Toward Improved Environmental Stability of Polymer:Fullerene and Polymer:Nonfullerene Organic

View Article Online
DOI: 10.1039/D5TC03779D

Solar Cells: A Common Energetic Origin of Light- and Oxygen-Induced Degradation. *ACS Energy Letters* **4**, 846-852 (2019).

30 E. T. Hoke, I. T. Sachs-Quintana, M. T. Lloyd, I. Kauvar, W. R. Mateker, A. M. Nardes, C. H. Peters, N. Kopidakis & M. D. McGehee. The Role of Electron Affinity in Determining Whether Fullerenes Catalyze or Inhibit Photooxidation of Polymers for Solar Cells. *Advanced Energy Materials* **2**, 1351-1357 (2012).

31 Y. Li, K.-K. Liu, F. R. Lin & A. K.-Y. Jen. Improving the Stability of Organic Solar Cells: From Materials to Devices. *Solar RRL* **7**, 2300531 (2023).

32 A. Tournebize, A. Rivaton, H. Peisert & T. Chassé. The Crucial Role of Confined Residual Additives on the Photostability of P3HT:PCBM Active Layers. *The Journal of Physical Chemistry C* **119**, 9142-9148 (2015).

33 M. Qin, P. Cheng, J. Mai, T.-K. Lau, Q. Zhang, J. Wang, C. Yan, K. Liu, C.-J. Su, W. You, X. Lu & X. Zhan. Enhancing Efficiency and Stability of Organic Solar Cells by UV Absorbent. *Solar RRL* **1**, 1700148 (2017).

34 V. Turkovic, S. Engmann, N. Tsierkezos, H. Hoppe, M. Madsen, H.-G. Rubahn, U. Ritter & G. Gobsch. Long-term stabilization of organic solar cells using UV absorbers. *Journal of Physics D: Applied Physics* **49**, 125604 (2016).

35 Y. Cui, Z. Chen, P. Zhu, W. Ma, H. Zhu, X. Liao & Y. Chen. Enhancing photostability and power conversion efficiency of organic solar cells by a “sunscreen” ternary strategy. *Science China Chemistry* **66**, 1179-1189 (2023).

36 N. Gasparini, M. Salvador, S. Strohm, T. Heumueller, I. Levchuk, A. Wadsworth, J. H. Bannock, J. C. de Mello, H.-J. Egelhaaf, D. Baran, I. McCulloch & C. J. Brabec. Burn-in Free Nonfullerene-Based Organic Solar Cells. *Advanced Energy Materials* **7**, 1700770 (2017).

37 H. Cha, J. Wu, A. Wadsworth, J. Nagitta, S. Limbu, S. Pont, Z. Li, J. Searle, M. F. Wyatt, D. Baran, J.-S. Kim, I. McCulloch & J. R. Durrant. An Efficient, “Burn in” Free Organic Solar Cell Employing a Nonfullerene Electron Acceptor. *Advanced Materials* **29**, 1701156 (2017).

38 Y. Wang, J. Luke, A. Privitera, N. Rolland, C. Labanti, G. Londi, V. Lemaur, D. T. W. Toolan, A. J. Sneyd, S. Jeong, D. Qian, Y. Olivier, L. Sorace, J.-S. Kim, D. Beljonne, Z. Li & A. J. Gillett. The critical role of the donor polymer in the stability of high-performance non-fullerene acceptor organic solar cells. *Joule* **7**, 810-829 (2023).

Open Access Article. Published on 23 December 2025. Downloaded on 1/20/2026 8:25:53 AM.
This article is licensed under a Creative Commons Attribution 3.0 Unported Licence.

Journal of Materials Chemistry C Accepted Manuscript

View Article Online
DOI: 10.1039/D5TC03779D

Open Access Article. Published on 23 December 2025. Downloaded on 1/20/2026 8:25:53 AM.
This article is licensed under a Creative Commons Attribution 3.0 Unported Licence.

Journal of Materials Chemistry C Accepted Manuscript

39 I. V. Martynov, L. N. Inasaridze & P. A. Troshin. Resist or Oxidize: Identifying Molecular Structure–Photostability Relationships for Conjugated Polymers Used in Organic Solar Cells. *ChemSusChem* **15**, e202101336 (2022).

40 T. Liu, Q. C. Burlingame, M. R. Ivancevic, X. Liu, J. Hu, B. P. Rand & Y.-L. Loo. Photochemical Decomposition of Y-Series Non-Fullerene Acceptors Is Responsible for Degradation of High-Efficiency Organic Solar Cells. *Advanced Energy Materials* **13**, 2300046 (2023).

41 A. Preobrajenski, A. Generalov, G. Ohrwall, M. Tchaplyguine, H. Tarawneh, S. Appelfeller, E. Frampton & N. Walsh. FlexPES: a versatile soft X-ray beamline at MAX IV Laboratory. *Journal of Synchrotron Radiation* **30**, 831-840 (2023).

42 N. Fairley, V. Fernandez, M. Richard-Plouet, C. Guillot-Deudon, J. Walton, E. Smith, D. Flahaut, M. Greiner, M. Biesinger, S. Tougaard, D. Morgan & J. Baltrusaitis. Systematic and collaborative approach to problem solving using X-ray photoelectron spectroscopy. *Applied Surface Science Advances* **5**, 100112 (2021).

43 J. H. Scofield. Hartree-Slater subshell photoionization cross-sections at 1254 and 1487 eV. *Journal of Electron Spectroscopy and Related Phenomena* **8**, 129-137 (1976).

44 A. Proctor & P. M. A. Sherwood. Data analysis techniques in x-ray photoelectron spectroscopy. *Analytical Chemistry* **54**, 13-19 (1982).

45 S. Hüfner. in *Photoelectron Spectroscopy: Principles and Applications* (ed Stefan Hüfner) 1-60 (Springer Berlin Heidelberg, 2003).

46 P. Urbánek, I. Kuřitka, J. Ševčík, J. Toušková, J. Toušek, V. Nádaždy, P. Nádaždy, K. Végsö, P. Šiffalovič, R. Rutsch & M. Urbánek. An experimental and theoretical study of the structural ordering of the PTB7 polymer at a mesoscopic scale. *Polymer* **169**, 243-254 (2019).

47 Y. Liu, K. Zhou, X. Zhou, W. Xue, Z. Bi, H. Wu, Z. Ma & W. Ma. Strengthening the Intermolecular Interaction of Prototypical Semicrystalline Conjugated Polymer Enables Improved Photocurrent Generation at the Heterojunction. *Macromolecular Rapid Communications* **43**, 2100871 (2022).

48 Y. W. Soon, H. Cho, J. Low, H. Bronstein, I. McCulloch & J. R. Durrant. Correlating triplet yield, singlet oxygen generation and photochemical stability in polymer/fullerene blend films. *Chemical Communications* **49**, 1291-1293 (2013).

49 M. Manceau, E. Bundgaard, J. E. Carlé, O. Hagemann, M. Helgesen, R. Søndergaard, M. Jørgensen & F. C. Krebs. Photochemical stability of π-conjugated polymers for

View Article Online
DOI: 10.1039/D5TC03779D

polymer solar cells: a rule of thumb. *Journal of Materials Chemistry* **21**, 4132-4141 (2011).

50 J. B. Patel, P. Tiwana, N. Seidler, G. E. Morse, O. R. Lozman, M. B. Johnston & L. M. Herz. Effect of Ultraviolet Radiation on Organic Photovoltaic Materials and Devices. *ACS Applied Materials & Interfaces* **11**, 21543-21551 (2019).

51 A. Classen, T. Heumueller, I. Wabra, J. Gerner, Y. He, L. Einsiedler, N. Li, G. J. Matt, A. Osvet, X. Du, A. Hirsch & C. J. Brabec. Revealing Hidden UV Instabilities in Organic Solar Cells by Correlating Device and Material Stability. *Advanced Energy Materials* **9**, 1902124 (2019).

52 J. Bertrandie, J. Han, C. S. P. De Castro, E. Yengel, J. Gorenflot, T. Anthopoulos, F. Laquai, A. Sharma & D. Baran. The Energy Level Conundrum of Organic Semiconductors in Solar Cells. *Advanced Materials* **34**, 2202575 (2022).

53 T. Shan, Y. Zhang, Y. Wang, Z. Xie, Q. Wei, J. Xu, M. Zhang, C. Wang, Q. Bao, X. Wang, C.-C. Chen, J. Huang, Q. Chen, F. Liu, L. Chen & H. Zhong. Universal and versatile morphology engineering via hot fluorous solvent soaking for organic bulk heterojunction. *Nature Communications* **11**, 5585 (2020).

54 S. H. K. Paleti, S. Hultmark, J. Han, Y. Wen, H. Xu, S. Chen, E. Järsvall, I. Jalan, D. R. Villalva, A. Sharma, J. I. Khan, E. Moons, R. Li, L. Yu, J. Gorenflot, F. Laquai, C. Müller & D. Baran. Hexanary blends: a strategy towards thermally stable organic photovoltaics. *Nature Communications* **14**, 4608 (2023).

55 J. Coates. Interpretation of infrared spectra, a practical approach. *Encyclopedia of analytical chemistry* **12**, 10815-10837 (2000).

56 I. E. Brumboiu, L. K. E. Ericsson, V. Blazinic, R. Hansson, A. Opitz, B. Brena & E. Moons. Photooxidation of PC60BM: new insights from spectroscopy. *Physical Chemistry Chemical Physics* **24**, 25753-25766 (2022).

57 S. Chambon, A. Rivaton, J.-L. Gardette & M. Firon. Photo- and thermal degradation of MDMO-PPV:PCBM blends. *Solar Energy Materials and Solar Cells* **91**, 394-398 (2007).

58 J. Guo, Y. Wu, R. Sun, W. Wang, J. Guo, Q. Wu, X. Tang, C. Sun, Z. Luo, K. Chang, Z. Zhang, J. Yuan, T. Li, W. Tang, E. Zhou, Z. Xiao, L. Ding, Y. Zou, X. Zhan, C. Yang, Z. Li, C. J. Brabec, Y. Li & J. Min. Suppressing photo-oxidation of non-fullerene acceptors and their blends in organic solar cells by exploring material design and employing friendly stabilizers. *Journal of Materials Chemistry A* **7**, 25088-25101 (2019).

Open Access Article. Published on 23 December 2025. Downloaded on 1/20/2026 8:25:53 AM.
This article is licensed under a Creative Commons Attribution 3.0 Unported Licence.

Journal of Materials Chemistry C Accepted Manuscript

View Article Online
DOI: 10.1039/D3TC03779D

59 J. Zhang, J. Guan, Y. Zhang, S. Qin, Q. Zhu, X. Kong, Q. Ma, X. Li, L. Meng, Y. Yi, J. Zheng & Y. Li. Direct Observation of Increased Free Carrier Generation Owing to Reduced Exciton Binding Energies in Polymerized Small-Molecule Acceptors. *The Journal of Physical Chemistry Letters* **13**, 8816-8824 (2022).

60 M. Nuber, L. V. Spanier, S. Roth, G. N. Vayssilov, R. Kienberger, P. Müller-Buschbaum & H. Iglev. Picosecond Charge-Transfer-State Dynamics in Wide Band Gap Polymer–Non-Fullerene Small-Molecule Blend Films Investigated via Transient Infrared Spectroscopy. *The Journal of Physical Chemistry Letters* **13**, 10418-10423 (2022).

61 D. Neusser, B. Sun, W. L. Tan, L. Thomsen, T. Schultz, L. Perdigón-Toro, N. Koch, S. Shoaee, C. R. McNeill, D. Neher & S. Ludwigs. Spectroelectrochemically determined energy levels of PM6:Y6 blends and their relevance to solar cell performance. *Journal of Materials Chemistry C* **10**, 11565-11578 (2022).

Open Access Article. Published on 23 December 2025. Downloaded on 1/20/2026 8:25:53 AM.
This article is licensed under a Creative Commons Attribution 3.0 Unported Licence.

Journal of Materials Chemistry C Accepted Manuscript

View Article Online
DOI: 10.1039/D5TC03779D

Role of the PM6 donor on the light-induced degradation of Y6 non-fullerene acceptors in PM6:Y6 blend films

Suraj Prasad, C. Moyses Araujo, Ellen Moons*

Department of Engineering and Physics, Karlstad University, SE-65188 Karlstad, Sweden.

** Corresponding author (e-mail: ellen.moons@kau.se)*

Open Access Article. Published on 23 December 2025. Downloaded on 1/20/2026 8:25:53 AM.
This article is licensed under a Creative Commons Attribution 3.0 Unported Licence.

Journal of Materials Chemistry C Accepted Manuscript

Data availability statement

The data supporting this article have been included as part of the Supplementary Information file.